Economic Geology, v. 108, pp. 365–377

PRIMARY ORIGIN OF MARGINAL Ni-Cu-(PGE) MINERALIZATION IN LAYERED INTRUSIONS: $\Delta^{33}S$ EVIDENCE FROM THE PLATREEF, BUSHVELD, SOUTH AFRICA

E. R. Sharman,[1,†] S. C. Penniston-Dorland,[2] J. A. Kinnaird,[3] P. A. M. Nex,[4] M. Brown,[2] and B. A. Wing[1]

[1] *Department of Earth & Planetary Sciences and GEOTOP, McGill University, Montréal, Quebec H3A 2A7, Canada*

[2] *Geology Department, University of Maryland, College Park, Maryland 20742*

[3] *School of Geosciences, University of the Witwatersrand, Johannesburg, South Africa*

[4] *Umbono Financial Services, Johannesburg, South Africa*

Abstract

The margins of layered igneous intrusions can host ore deposits of nickel, copper, and platinum group elements (PGEs). These marginal deposits are characterized by a complex geologic history, which obscures direct evidence for the mineralization process. Mass-independent fractionation of sulfur isotopes is a distinguishing feature of Archean sedimentary rocks, and reflects processes operating solely in the Archean surface environment. As a result, mass-independent fractionation of sulfur isotopes is a chemically conservative tracer that indicates the involvement of crustal sulfur in marginal Ni-Cu-(PGE) deposits. In this study we use mass-independent fractionation of sulfur isotopes to evaluate the sulfur budget of the Platreef—the marginal PGE-bearing horizon of the northern limb of the Bushveld Complex, South Africa. Our multiple sulfur isotope measurements demonstrate that crustal sulfur in the Platreef originated from a restricted stratigraphic horizon (the Duitschland Formation) in the Platreef footwall. As this signature is spread out over the ≈100-km strike length of the Platreef, it does not reflect sulfur inputs from the local footwall. Nonlocal crustal sulfur isotope anomalies are unexpected given the high metal tenors in the Platreef. These features can be reconciled if a preformed Ni-Cu-(PGE)–rich sulfide melt assimilated sulfur in a staging chamber bounded completely by the Duitschland Formation, and then was emplaced into the Platreef. Such a model is supported by long-standing observations of lithologic, geochemical, and stratigraphic similarities between the Merensky Reef and the Platreef, as well as by recent suggestions that the northern limb represents an "escape structure" for the rest of the Bushveld Complex. Crustal sulfur assimilation is often thought to initiate the ore-forming process by producing an immiscible sulfide melt that can collect base metals and PGEs. In the Platreef, however, crustal sulfur assimilation apparently diluted a preexisting PGE-rich sulfide melt instead.

Introduction

Immiscible sulfide liquids are a critical component of the standard model for the formation of magmatic base metal and platinum group element (PGE) deposits (Mungall and Naldrett, 2008). The base metals and PGEs strongly partition into sulfide melts relative to coexisting silicate melts (Fleet et al., 1999), initiating the enrichment process that leads to the formation of ore deposits. Representative models exist for the physical mechanisms that control the macroscale and microscale extraction of base metals and PGEs from silicate magmas (Campbell and Naldrett, 1979; Mungall, 2002; Kerr and Leitch, 2005). However, the local geologic setting strongly influences our understanding of the processes behind the original sulfide saturation of a particular silicate melt, as well as the segregation and collection of enriched sulfide melt into a specific ore deposit (Naldrett, 2004).

Local contingencies are especially important for accumulations of Ni-Cu-(PGE)–rich sulfides at the margins of layered intrusions. Marginal accumulations are defined by their complicated physical and chemical relationships to the wall rock surrounding the intrusion (Naldrett, 2010). They typically host abundant xenolith populations, may record multiple intrusive pulses, and preserve clear evidence of hydrothermal material transfer across intrusion-wall rock contacts (Kinnaird et al., 2005; Hutchinson and McDonald, 2008; Penniston-Dorland et al., 2008). These features obscure the origins of sulfide mineralization in marginal settings.

Measurements of the two most common sulfur isotopes—^{34}S and ^{32}S—offer a way to disentangle the effects of sulfide processing before, during, and after the emplacement of an immiscible sulfide melt in marginal deposits. Variations in ^{34}S-^{32}S ratios of sedimentary wall rocks can be more than an order of magnitude larger than the sulfur isotope variations of mantle-derived magmatic sulfur (Seal, 2006). Ratios of ^{34}S-^{32}S can track the role of crustal sulfur in driving the initial sulfide saturation of a silicate melt, as well as any exchange between crustal sulfur and the immiscible sulfide melt after it formed. This approach has been successfully applied to basal and marginal mineralization in layered intrusions (e.g., Duluth and Norilsk; Ripley and Li, 2003). However, $^{34}S/^{32}S$ measurements can often provide an equivocal view of the role of crustal sulfur in marginal deposits. The susceptibility of ^{34}S-^{32}S ratios to modification by magmatic (Ripley and Li, 2003) and hydrothermal processes (Penniston-Dorland et al., 2008) and the limited sulfur isotope variability in many Proterozoic and Archean sedimentary wall rocks (Ripley and Li, 2003) both contribute to this mixed message. Here, we show that consideration of a third sulfur isotope, ^{33}S, can provide a definitive and sensitive tool for identifying crustal sulfur contributions, even in the complicated multistage geologic setting of the Platreef (an archetypal and well-endowed marginal Ni-Cu-(PGE) deposit; Naldrett et al., 2008) of the Bushveld Igneous Complex, South Africa.

† Corresponding author: e-mail, libbysh@gmail.com

Submitted: September 8, 2011
Accepted: July 8, 2012

Multiple Sulfur Isotopes and Magmatic Ore Deposits

During the Archean (>2.5 Ga), lack of an oxygenated atmosphere likely allowed for the anomalous fractionation of sulfur isotopes during atmospheric photochemical reactions (Farquhar et al., 2001). The magnitude of this anomalous isotopic fractionation can be characterized by the measurement of $\delta^{33}S$ values ($\delta^{33}S = [(^{33}S/^{32}S)_{sample}/(^{33}S/^{32}S)_{standard} - 1] \times 1{,}000$) in addition to $\delta^{34}S$ values ($\delta^{34}S = [(^{34}S/^{32}S)_{sample}/(^{34}S/^{32}S)_{standard} - 1] \times 1{,}000$), and is indicated by nonzero $\Delta^{33}S$ values ($= \delta^{33}S_{measured} - \delta^{33}S_{predicted}$, where $\delta^{33}S_{predicted} = [(\delta^{34}S_{measured} + 1)^{0.515} - 1] \times 1{,}000$). While the proposed atmospheric origin of anomalous $\Delta^{33}S$ values in the ancient rock record is under active research (cf. Lyons, 2007; Danielache et al., 2008; Watanabe et al., 2009), all working models for the Archean sulfur cycle consider anomalous (or "mass independent") sulfur isotope fractionation to be a surface process. A nonzero $\Delta^{33}S$ value, therefore, indicates the presence of sulfur that cycled through the Archean surface environment (Farquhar and Wing, 2003). Preservation of nonzero $\Delta^{33}S$ values through geologic S processing (e.g., metamorphism, crustal assimilation) should occur with high fidelity—even in the face of significant mass-dependent $\delta^{34}S$ fractionation—unless mixing processes dilute the $\Delta^{33}S$ signature.

Because of their chemically conservative behavior, $\Delta^{33}S$ values can directly track the incorporation of Archean crustal sulfur into a mineralizing system, as well as monitor any subsequent mixing with primitive mantle-derived sulfur ($\Delta^{33}S \approx 0.00 \pm 0.03‰$ based on analyses of peridotite xenoliths [Farquhar et al., 2002] and sulfide inclusions in peridotitic and eclogitic diamonds [Cartigny et al., 2009], and basalts derived from mantle sources [Ono et al., 2007; Rouxel et al., 2008; Peters et al., 2010]). Recent studies have exploited these properties to examine ore-forming processes and ore prospectivity in complicated mineralization environments (Jamieson et al., 2006; Penniston-Dorland et al., 2008; Bekker et al., 2009; Fiorentini et al., 2012; Ding et al., in press). In one example, $\Delta^{33}S$ measurements indicate that komatiite-hosted deposits of Mount Keith, Western Australia, required cannibalization of preexisting hydrothermal and sedimentary sulfide accumulations by metal-rich, sulfur-poor komatiite melts (Bekker et al., 2009). In another, nonzero $\Delta^{33}S$ values in ore sulfides from the Selebi-Phikwe greenstone belt, Botswana, preserve a memory of sulfur saturation via assimilation of crustal sulfur, even though the surrounding gneisses appear to have lost most of their sulfur through metamorphic devolatilization after ore formation (Fiorentini et al., 2012). These examples suggest that multiple sulfur isotopes will be a fruitful forensic tool for Ni-Cu-(PGE) deposits at the margins of layered intrusions.

Geologic Background

The northern limb of the Bushveld Igneous Complex, South Africa, is a 110-km-long, slightly sinuous, NW-striking, layered intrusive igneous sequence (Armitage et al., 2002). It is typically divided into southern, central, and northern sectors (Fig. 1). The Platreef is a magmatic Ni-Cu-(PGE) deposit in the northern limb. It is the third largest PGE deposit in the world, after two other PGE horizons within the eastern and western lobes of the Bushveld (Naldrett et al., 2011). The Platreef occurs at the base of the igneous sequence in the northern limb, in contact with the underlying footwall rocks. The Platreef has a nonconformable, transgressive relationship with its footwall, which places it in contact with rocks that young to the south (Fig. 1).

The Platreef is a highly heterogeneous body (Kinnaird, 2005), composed of pyroxenite, feldspathic pyroxenite (pyroxenites with >10% interstitial plagioclase), gabbronorite, and norite, as well as altered versions of these rocks (serpentinite), and physical mixtures of these rocks with highly altered rocks of the Platreef footwall ("para-pyroxenites"). The footwall is composed of Archean granites in the far north, followed in the south by members of the 2.67 to 2.07 Ga Transvaal Supergroup sedimentary sequence (Coetzee, 2001; Eriksson et al., 2001). These members comprise, from north to south, the Malmani Subgroup (limestone, chert-rich, and chert-poor dolomite), the Penge Formation (predominantly quartz-, magnetite-, and hematite-rich rocks interlayered with minor carbonaceous shale beds), the Duitschland Formation (dominated by fine-grained laminated shales and marls with thick dolomite beds more common in the upper part of the formation), and the Timeball Hill Formation (Fig. 1). The Platreef also contains xenoliths of altered footwall rocks, including hornfels rafts that most likely have shale protoliths, and calc-silicate rafts, which were derived from dolomites (Sharman-Harris et al., 2005; Johnson et al., 2010).

The base and precious metal mineralization of the Platreef is unevenly distributed and occurs over a zone that is up to 400 m thick. Sulfide minerals occur throughout the succession and are generally centimeter- to millimeter-sized blebs and interstitial grains of pentlandite, pyrrhotite, and chalcopyrite. A wide range of accessory sulfide minerals is also present, including sphalerite, galena, molybdenite, pyrite, chalcocite, and covellite (Hutchinson and Kinnaird, 2005; Holwell et al., 2007). In some locations, zones of massive chalcopyrite are found close to the footwall contact. Sulfide mineralization also occurs in the metamorphosed footwall of the Platreef. PGE mineralization is generally associated with sulfide mineralization, though postemplacement hydrothermal remobilization of the PGEs has been proposed (Hutchinson and McDonald, 2008).

Conventional sulfur isotope analyses have led to conflicting views on the role of crustal sulfur in the formation of the Platreef. Some Platreef $\delta^{34}S$ values fall outside the range expected for a mantle-derived magma ($\delta^{34}S \approx 0 \pm 2‰$; Seal, 2006), leading to the suggestion that xenoliths and local wall rocks released sulfur during postemplacement contact metamorphism and triggered sulfide saturation within the Platreef parental melt (Buchanan et al., 1981; Buchanan and Rouse, 1984; Manyeruke et al., 2005; Sharman-Harris et al., 2005). Other $\delta^{34}S$ values fall within the mantle-derived range, suggesting that the formation of Platreef ore resulted from magmatic segregation of sulfide from a PGE-enriched mantle-derived melt (Liebenberg, 1968; Hulbert, 1983; Barton et al., 1986; Holwell and McDonald, 2006). Both hypotheses may have validity if early-formed sulfides (with near-zero $\delta^{34}S$ values) reflect sulfur saturation of the Platreef magma prior to intrusion, while later-formed sulfides (exhibiting a wider range of $\delta^{34}S$ values) reflect contamination by footwall material on a strictly local scale (Holwell et al., 2007).

Such local mass transfer of sulfur across the Platreef-footwall contact was documented by a recent multiple sulfur

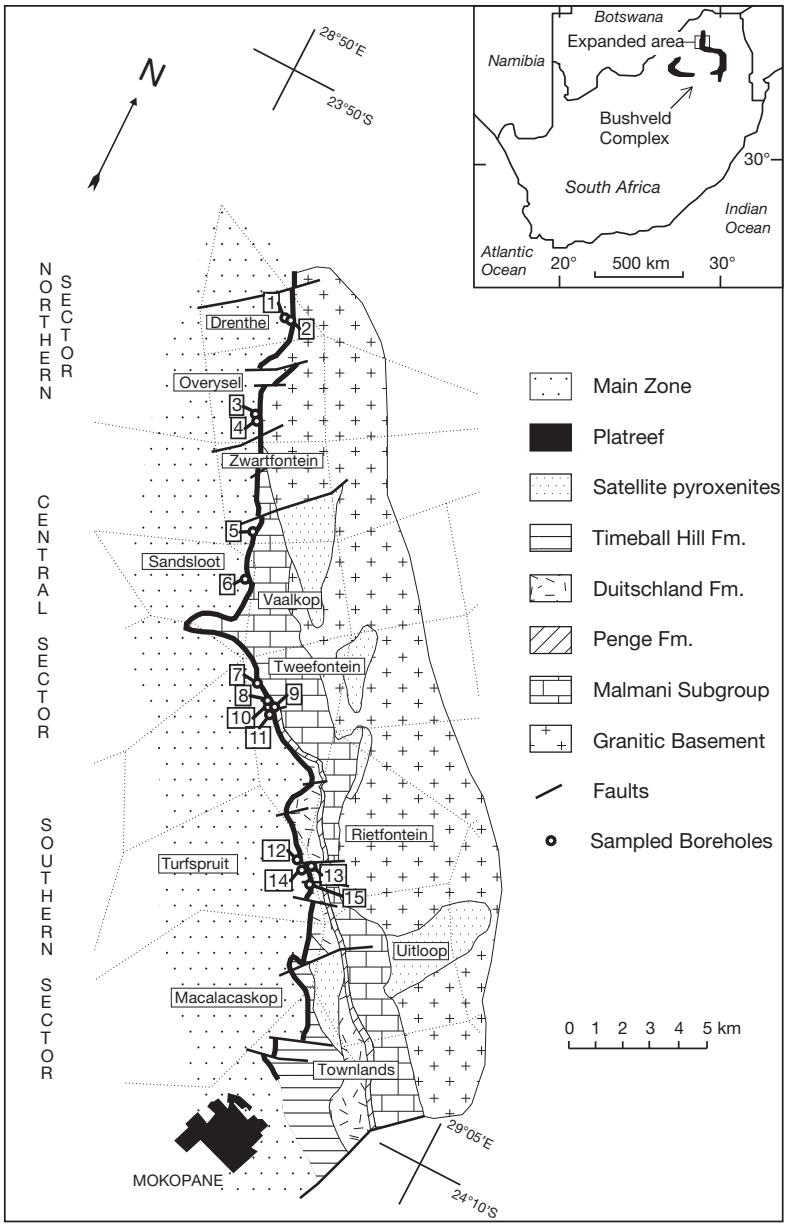

FIG. 1. Geologic map of the Platreef showing farm boundaries and sampled borehole locations. Boreholes: 1 = PR-175, 2 = PR-174, 3 = OY-405, 4 = OY-518, 5 = ZN-259*, 6 = SS-315*, 7 = TN-31*, 8 = TN-188, 9 = TN-92, 10 = TN-190D1*, 11 = TN-192D1, TN-194*, 12 = ATS-46, 13 = ARF-08, 14 = ATS-57, 15 = ITS054 (*from Penniston-Dorland et al., 2008).

isotope investigation (Penniston-Dorland et al., 2008). At the locations studied in detail (farms Tweefontein and Sandsloot), sulfur carrying near-zero $\Delta^{33}S$ values was transported, probably through advection of hydrothermal fluids, from the Platreef into the surrounding wall rocks. A small contribution of footwall sulfur to the Platreef sulfides accompanied this process, probably associated with back diffusion against the overall advection of sulfur out of the Platreef. This contact enrichment within the Platreef is limited to ≈5 m from the footwall contact, and was therefore not a major trigger of sulfide mineralization (Penniston-Dorland et al., 2008). In this study we use $\Delta^{33}S$ analyses to evaluate this hypothesis along the full ≈100 km strike length of the Platreef.

Analytical Methods

Samples for this study were taken from diamond drill hole cores from the northern (farms Overysel and Drenthe), central (farms Tweefontein, Sandsloot, and Zwartfontein) and southern (farms Turfspruit and Rietfontein) sectors of the Platreef (Fig. 1; Table 1), and were chosen to encompass as many different footwall rock types and varying distances from the footwall contact as possible. Sulfur isotope analyses of selected samples were conducted using either whole-rock samples or sulfide mineral separates. Analyses of multiple sulfur isotopes were conducted at the University of Maryland. Sulfide mineral separates were converted to SF_6 gas by laser

TABLE 1. Multiple Sulfur Isotope Data

Sample no.	Farm	Depth (m)	Description	Sample type	$\delta^{33}S$ (‰)	$\delta^{34}S$ (‰)	$\Delta^{33}S$ (‰)
			Platreef ore sulfides				
	Northern sector						
PR174/21.50	Drenthe	21.50	Feldspathic pyroxenite	WR	2.19	3.74	0.27
PR174/88.50	Drenthe	88.50	Contaminated norite	WR	2.74	4.66	0.34
PR174/106.13	Drenthe	106.13	Serp. pyroxenite	WR	2.61	4.50	0.29
PR174/207.50	Drenthe	207.50	Granofels	WR	1.24	1.89	0.27
PR174/240.50	Drenthe	240.50	Serpentinite	WR	1.48	2.29	0.30
PR175/77.18	Drenthe	77.18	Feldspathic pyroxenite	WR	3.06	5.24	0.36
PR175/102.50	Drenthe	102.50	Feldspathic pyroxenite	WR	5.56	10.53	0.15
PR175/116.81	Drenthe	116.81	Feldspathic pyroxenite	WR	2.95	5.14	0.31
OY405/102A	Overysel	404.55	Pyroxenite	Po/Pnt	2.60	4.64	0.21
OY405/102B	Overysel	404.55	Pyroxenite	Cp	4.65	8.58	0.24
OY405/102C	Overysel	404.55	Pyroxenite	Sulf	2.34	4.05	0.26
OY405/189A	Overysel	460.82	Serp. pyroxenite	Cp	2.60	4.71	0.18
OY405/189B	Overysel	460.82	Serp. pyroxenite	Sulf	1.98	3.42	0.23
OY518/14	Overysel	—	Pyroxenite	Sulf	3.11	5.51	0.27
OY518/51	Overysel	—	Pyroxenite	Sulf	2.53	4.44	0.25
OY518/126	Overysel	—	Pyroxenite	Sulf	1.17	2.07	0.10
	Central sector						
[1]SS315/5	Sandsloot	49.60	Feldspathic pyroxenite	WR	2.32	4.01	0.26
[1]SS315/11	Sandsloot	102.80	Feldspathic pyroxenite	WR	4.66	8.77	0.15
[1]SS315/14	Sandsloot	131.50	Feldspathic pyroxenite	WR	4.96	9.20	0.23
[1]SS315/6A	Sandsloot	144.80	Feldspathic pyroxenite	WR	4.04	6.94	0.47
[1]SS315/18	Sandsloot	147.10	Feldspathic pyroxenite	WR	4.77	8.44	0.44
[1]SS315/18A	Sandsloot	147.10	Feldspathic pyroxenite	Po	4.73	8.36	0.43
[1]SS315/18B	Sandsloot	147.10	Feldspathic pyroxenite	Po	4.74	8.36	0.44
[1]SS315/18C	Sandsloot	147.10	Feldspathic pyroxenite	Cp	4.86	8.60	0.44
[1]SS315/19	Sandsloot	148.70	Feldspathic pyroxenite	WR	4.84	8.34	0.55
[1]SS315/19A	Sandsloot	148.70	Feldspathic pyroxenite	Po	4.75	8.39	0.44
[1]SS315/19B	Sandsloot	148.70	Feldspathic pyroxenite	Po	4.86	8.68	0.40
[1]SS315/19C	Sandsloot	148.70	Feldspathic pyroxenite	Cp	3.95	7.19	0.25
[1]SS315/20	Sandsloot	149.60	Feldspathic pyroxenite	WR	4.79	8.45	0.45
[1]SS315/21	Sandsloot	150.80	Feldspathic pyroxenite	WR	4.73	8.24	0.49
[1]SS315/22	Sandsloot	151.50	Feldspathic pyroxenite	WR	4.52	8.17	0.32
[1]TN190D1/74	Tweefontein	130.20	Pyroxenite	Po	1.93	3.44	0.16
[1]TN190D1/167	Tweefontein	196.00	Pyroxenite	Po	2.18	3.78	0.23
[1]TN190D1/109	Tweefontein	206.20	Norite	Po	1.61	3.07	0.03
[1]TN190D1/139	Tweefontein	314.70	Pyroxenite	Po	1.56	2.74	0.15
[1]TN190D1/22	Tweefontein	331.30	Leuconorite	Po	2.50	4.54	0.16
[1]TN190D1/2-2	Tweefontein	335.00	Pyroxenite	WR	3.56	6.73	0.09
[1]TN190D1/56A	Tweefontein	336.90	Pyroxenite	Po	3.14	5.86	0.13
[1]TN190D1/56B	Tweefontein	336.90	Pyroxenite	Cp	3.47	6.59	0.09
[1]TN190D1/2-1	Tweefontein	338.20	Leuconorite	WR	5.31	10.14	0.10
[1]TN190D1/149	Tweefontein	343.90	Serpentinite	Po	5.97	11.40	0.12
TN92/199A	Tweefontein	—	Pyroxenite	Cp	4.23	8.10	0.06
TN92/199B	Tweefontein	—	Pyroxenite	Sulf	4.43	8.45	0.08
TN92/228A	Tweefontein	—	Pyroxenite	Po/Pnt	6.65	12.70	0.13
TN92/228B	Tweefontein	—	Pyroxenite	Cp	5.98	11.44	0.10
TN192D13/10A	Tweefontein	—	Pyroxenite	Po	3.12	5.87	0.10
TN192D13/10B	Tweefontein	—	Pyroxenite	Po	3.13	5.84	0.12
TN192D13/10C	Tweefontein	—	Pyroxenite	Cp	3.24	6.06	0.12
	Southern sector						
ATS 46/60.34	Turfspruit	60.34	Pegmatoidal norite	Cp	1.24	2.03	0.19
ATS 46/461.21	Turfspruit	461.21	Feldspathic pyroxenite	Po	3.09	5.22	0.41
ATS 57/72.48	Turfspruit	72.48	Pyroxenite	Po	0.82	1.25	0.17
ATS 57/219.26	Turfspruit	219.26	Pyroxenite	Po	3.20	5.30	0.47
ATS 57/221.39	Turfspruit	221.39	Pyroxenite	Cp	3.82	6.32	0.57
ATS 57/221.39	Turfspruit	221.39	Pyroxenite	Po	3.38	5.49	0.56
ITS054/22	Turfspruit	22.12	Feldspathic pyroxenite	WR	0.89	1.43	0.15
ITS054W/198	Turfspruit	197.91	Serpentinite	WR	3.07	4.93	0.53
ITS054W/226A	Turfspruit	225.85	Melanorite	WR	3.39	5.45	0.58
ITS054W/230	Turfspruit	229.8	Melanorite	WR	3.73	6.15	0.57
ITS054W/274	Turfspruit	273.88	Feldspathic pyroxenite	WR	3.35	5.81	0.37
ARF 08/49.26	Rietfontein	49.26	Norite	Po	2.94	4.84	0.45
ARF 08/124.64	Rietfontein	124.64	Massive sulfide	Po	3.11	5.17	0.46
ARF 08/124.64	Rietfontein	124.64	Massive sulfide	Po	3.83	6.43	0.53
ARF 08/129.78	Rietfontein	129.78	Norite	Po	3.20	5.30	0.47

TABLE 1. *(Cont.)*

Sample no.	Farm	Depth (m)	Description	Sample type	$\delta^{33}S$ (‰)	$\delta^{34}S$ (‰)	$\Delta^{33}S$ (‰)
			Footwall				
	Central sector						
[1]SS315/23	Sandsloot	159.10	Calc-silicate	WR	1.02	0.72	0.65
[1]SS315/25	Sandsloot	169.90	Calc-silicate	WR	5.62	8.23	1.39
[1]SS315/25A	Sandsloot	171.60	Calc-silicate	WR	3.73	4.62	1.35
[1]SS315/25B	Sandsloot	174.80	Calc-silicate	WR	5.08	5.77	2.11
[1]SS315/25C	Sandsloot	177.30	Calc-silicate	WR	6.11	5.29	3.39
[1]SS315/26	Sandsloot	179.30	Calc-silicate	WR	6.92	4.88	4.41
[1]SS315/27	Sandsloot	185.50	Calc-silicate	WR	8.15	6.07	5.04
[1]SS315/31	Sandsloot	214.60	Calc-silicate	WR	7.81	6.71	4.36
[1]SS315/38	Sandsloot	301.90	Calc-silicate	WR	6.23	5.60	3.35
[1]TN190D1/H1	Tweefontein	345.60	Hornfels	WR	9.62	18.10	0.34
[1]TN190D1/P2	Tweefontein	350.10	Calc-silicate	WR	3.29	6.08	0.17
[1]TN190D1/H2	Tweefontein	352.80	Hornfels	WR	–0.53	–1.08	0.03
[1]TN190D1/H3	Tweefontein	353.60	Hornfels	WR	0.11	0.04	0.09
[1]TN190D1/H6	Tweefontein	366.20	Hornfels	WR	–0.02	–0.85	0.41
[1]TN190D1/H7	Tweefontein	373.90	Hornfels	WR	0.00	–0.67	0.35
[1]TN190D1/H8	Tweefontein	374.90	Hornfels	WR	0.24	–0.26	0.38
[1]TN190D1/H9A	Tweefontein	381.80	Hornfels	WR	–7.31	–14.47	0.17
[1]TN190D1/H9C	Tweefontein	392.50	Hornfels	WR	1.03	0.59	0.72
[1]TN190D1/H10	Tweefontein	395.40	Hornfels	WR	1.73	1.57	0.93
[1]TN190D1/B1	Tweefontein	409.40	BIF	WR	8.90	15.83	0.78
[1]TN190D1/B2	Tweefontein	414.60	BIF	WR	3.03	4.40	0.77
[1]TN194/7	Tweefontein	—	Hornfels	WR	–5.34	–12.05	0.88
	Southern sector						
ATS 57/325.25	Turfspruit	325.25	Calc-silicate	Po	14.76	28.72	0.07
ATS 57/335.07	Turfspruit	335.07	Calc-silicate	Py	10.73	20.62	0.17
ITS054W/323	Turfspruit	323.2	Dolomite footwall	WR	9.28	17.97	0.06
ITS054W/341	Turfspruit	341.33	Dolomite footwall	WR	7.64	14.7	0.09
			Xenoliths				
	Northern sector						
PR175/19.08	Drenthe	19.08	Calc-silicate	WR	3.57	6.30	0.33
	Central sector						
[1]TN31/134	Tweefontein	—	Calc-silicate	Cp	3.11	3.94	1.09
[1]TN31/160	Tweefontein	—	Hornfels	WR	0.47	–4.08	2.58
TN188/H3	Tweefontein	221.20	Hornfels	WR	–0.08	–0.33	0.09
	Southern sector						
ITS054W/203	Turfspruit	203.4	Hornfels	WR	–10.72	–20.92	0.11
ITS054W/223	Turfspruit	223.29	Hornfels	WR	–4.44	–8.91	0.16
ITS054W/275	Turfspruit	274.53	Hornfels	WR	3.26	5.6	0.38

Notes: All isotope ratios reported relative to Vienna-Cañon Diablo Troilite; — = depth not measured, BIF = banded iron formation, Cp = Chalcopyrite, Pnt = Pentlandite, Po = Pyrrhotite, Py = pyrite, Serp = serpentinite, Sulf = sulfide, WR = whole rock

[1] Data from Penniston-Dorland et al., 2008

heating of separated sulfides under an F_2 atmosphere, following the methods of Hu et al. (2003). Whole-rock samples were crushed and then reacted with a Cr-reducing solution that allowed the liberation of H_2S gas (Canfield et al., 1986). This H_2S was subsequently converted to solid Ag_2S by trapping the H_2S in a zinc acetate solution and reacting the ZnS that precipitated with $AgNO_3$. The Ag_2S precipitate was then rinsed and dried before being reacted in a nickel vessel in the presence of excess F_2 to produce SF_6. The SF_6 resulting from both of the above procedures was purified first cryogenically and then by gas chromatography. Purified SF_6 was introduced to a ThermoFinnigan MAT 253 dual-inlet gas-source mass spectrometer, and sulfur isotope abundances were measured by monitoring the $^{32}SF_5^+$, $^{33}SF_5^+$, $^{34}SF_5^+$ ion beams at mass to charge ratios of 127, 128, and 129, respectively. Sulfur isotope measurements are reported relative to Vienna-Cañon Diablo Troilite (V-CDT). The isotopic composition of the international reference Ag_2S material IAEA-S-1 has a $\delta^{34}S$ value of –0.3‰ (Robinson, 1995). We take IAEA-S-1 to have a $\Delta^{33}S$ value of 0.094‰. The analytical reproducibility (1σ) for all samples is estimated to be ± 0.29‰ for $\delta^{34}S$ and ± 0.02‰ for $\Delta^{33}S$, based on the standard deviation of multiple analyses of an in-house pyrite standard (P1), conducted over a period of more than five years.

Results

Multiple sulfur isotope analyses in Table 1 and Figure 2 are from ore sulfides, footwall rocks, and xenoliths from the Platreef. Measured $\delta^{34}S$ values of Platreef ore sulfides range from 1 to 13‰, in agreement with many previous studies (Buchanan et al., 1981; Buchanan and Rouse, 1984; Manyeruke et al., 2005; Sharman-Harris et al., 2005). Compared to typical mantle compositions ($\delta^{34}S = 0 \pm 2$‰), they indicate that the mineralization process involved surface sulfur. Within all sectors of the Platreef, $\Delta^{33}S$ values of ore sulfides are positive and nonzero, ranging from 0.03 to 0.58‰. Nonzero $\Delta^{33}S$ values confirm the involvement of surface sulfur (i.e., sulfur that had been processed through the hydrosphere) in the mineralization of the Platreef.

There is regional variability in sulfur isotope composition. Most ore sulfides from the southern and northern sectors have distinctly lower $\delta^{34}S$ values than those from the central sector (Table 1; Fig. 2). There does not appear to be a strong control of sulfide mineralogy on $\delta^{34}S$ values. Fractionation between coexisting pyrrhotite/pentlandite and chalcopyrite ($\delta^{34}S_{ccp}$-$\delta^{34}S_{po}$) is <1‰ in four out of seven mineral pairs, negative in two out of seven pairs, and positive in the remaining pair (Table 1). Footwall rocks and xenolith samples span a much broader range of $\delta^{34}S$ values. Calc-silicates in the northern and central sectors have $\delta^{34}S$ values ranging from 0.7 to 8.2‰ and in the southern sector calc-silicates and dolomites have $\delta^{34}S$ values ranging from 14.7 to 28.7‰. Hornfels samples record the broadest range of $\delta^{34}S$ values, from –20.9 to 18.1‰, and include the only negative $\delta^{34}S$ values observed in the Platreef.

The ore sulfides from the southern and northern sectors have distinctly different $\Delta^{33}S$ values, with high $\Delta^{33}S$ values measured in rocks of the southern sector and lower $\Delta^{33}S$ values in rocks from the northern sector (Table 1; Fig. 2). The central sector spans almost the entire range of $\Delta^{33}S$ values measured in this study. The $\Delta^{33}S$ values for hornfels and calc-silicate footwall rocks and xenoliths show ≈10× more variation in $\Delta^{33}S$ values compared to ore sulfides, with values as high as 5.04‰. There is a broad correspondence between $\Delta^{33}S$ values from footwall rocks and xenoliths from the same location, with $\Delta^{33}S$ values from the central sector calc-silicate rocks exhibiting the largest magnitudes in the district.

Discussion

The nonzero $\Delta^{33}S$ values and the wide range in $\delta^{34}S$ values of the Platreef are consistent with significant contributions of sulfur from Archean supracrustal sources. Observations at different length scales constrain viable models for the incorporation of this sulfur into the Platreef mineralizing system. First, at the most local scale, comparison of $\Delta^{33}S$ values in

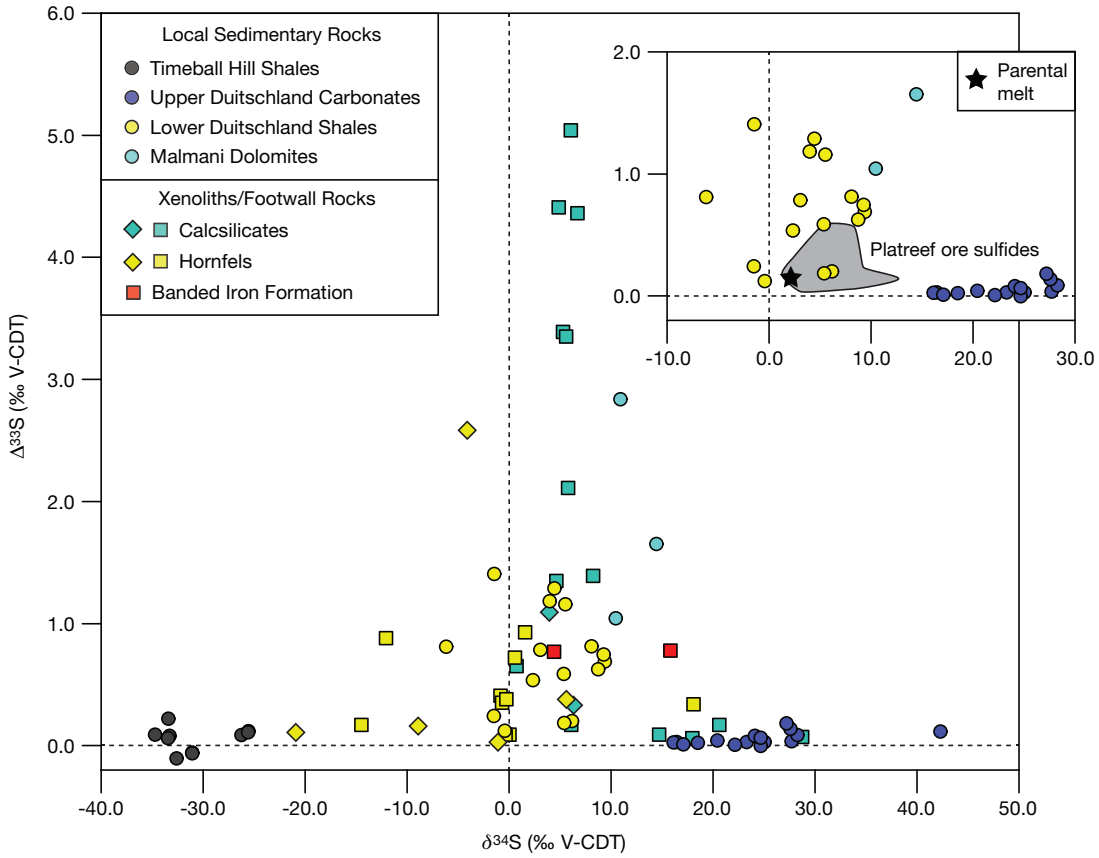

FIG. 2. Multiple sulfur isotope data for local sedimentary rocks of the Transvaal Supergroup and Platreef xenolith and footwall samples (data from this study; Bekker et al., 2004; Penniston-Dorland et al., 2008; Guo et al., 2009). Inset shows the field of $\Delta^{33}S$ and $\delta^{34}S$ values measured from the Platreef ore sulfides compared to multiple sulfur isotope measurements from likely sedimentary sulfur sources. Measurement uncertainty (1σ) is smaller than the size of the symbol.

Platreef sulfides and the local footwall illustrates whether the sulfur in the Platreef could have originated locally or whether it was brought in from some distal location. This analysis constrains the distance scale over which sulfur was potentially sourced. Second, regional-scale variations of $\Delta^{33}S$ and $\delta^{34}S$ values within the Platreef can be used to look for patterns consistent with the inferred direction of magma input to fingerprint the ultimate sources of the incorporated sulfur. Third, sourcing of sulfur from outside the Platreef is considered, in which case the multiple sulfur isotope compositions of the sulfides may record the full history of interaction between an immiscible sulfide melt that concentrated Platreef PGEs, the silicate melt that was the ultimate PGE source, and any exogenous sources of sulfur. We discuss each of these possibilities in the following subsections.

Spatial record of sulfur contamination

Observations of the contact between the Platreef igneous rocks and the footwall suggest relatively limited material exchange during emplacement, localized to thin zones at the contacts between the Platreef, the direct footwall, and footwall xenoliths (Sharman-Harris et al., 2005; Holwell et al., 2007; Penniston-Dorland et al., 2008). Direct incorporation of footwall sulfur, for example, seems to be limited to distances less than 5 m from the footwall contact (Penniston-Dorland et al., 2008). These characteristics suggest a pair of tests for evaluating whether purely local interactions are responsible for the sulfur isotope composition of the Platreef. Both tests rely on the chemically conservative nature of $\Delta^{33}S$ values, and are likely to be more restrictive than comparisons that also use associated $\delta^{34}S$ values.

The first test is whether $\Delta^{33}S$ values in ore sulfides far away (>5 m) from any footwall material or xenoliths are outside the range of $\Delta^{33}S$ for the presumed parental magma composition (0.11 ‰ < $\Delta^{33}S$ < 0.21‰; Penniston-Dorland et al., 2008). Samples that have $\Delta^{33}S$ above 0.21‰ and are far from the contact fail this test and must have had their multiple sulfur isotope composition set by some process other than local contact enrichment. Many of the Platreef ore sulfides have $\Delta^{33}S$ values that fall above this value. Because interpretations of these observations are complicated by the spatial heterogeneity of the xenoliths within the Platreef (Kinnaird et al., 2005) and the one-dimensional nature of our drill core samples, failing solely this test is not definitive.

A second test is to look for a correlation between the Platreef $\Delta^{33}S$ values at a given location with the associated footwall $\Delta^{33}S$ values. Once sulfur with a nonzero $\Delta^{33}S$ value is incorporated into a magma from the local footwall, igneous processes can only lead to lower overall $\Delta^{33}S$ values through dilution with primary magmatic sulfur. This property suggests that if nonzero $\Delta^{33}S$ values in the Platreef are due to interaction with local footwall rocks, the Platreef $\Delta^{33}S$ values should be equal to or less than that of local footwall rocks. On a comparative plot of $\Delta^{33}S_{Platreef}$ against $\Delta^{33}S_{Footwall}$, Platreef sulfide samples should not plot above a line with a slope of 1 (Fig. 3).

Platreef ore sulfides from farm Turfspruit (cores ATS-57 and ITS 054) have $\Delta^{33}S$ values of 0.58‰ occurring approximately 100 m from the contact with footwall rocks and xenoliths that have a maximum $\Delta^{33}S$ of 0.38‰, failing both tests. Platreef samples on farms Drenthe and Overysel have Archean granite as footwall, for which there are no measurements of $\Delta^{33}S$ values. If the $\Delta^{33}S$ values of these ancient granitic rocks are near zero, reflecting an igneous crustal source, the nonzero $\Delta^{33}S$ values (0.10 to 0.36‰) of the nearby Platreef rocks suggest nonlocal derivation of sulfur (Fig. 3). Alternatively, magmatic homogenization of an average crustal sedimentary source could yield granitic $\delta^{33}S$ values greater than nearby Platreef rocks (Fig. 3). Similar comparisons for Sandsloot, Tweefontein North, and Rietfontein indicate localized interaction is possible, though not required, for these localities (Fig. 3). As Platreef samples taken from some localities exhibit $\Delta^{33}S$ values that are higher than those of the direct footwall, incorporation of local footwall sulfur cannot be the sole mechanism by which the Platreef magma was enriched in sulfur. Sulfur from an additional, allochthonous crustal source must have been incorporated into the Platreef mineralizing system at some point during its evolution.

Regional sources of sulfur

Because the data suggest sulfur is not sourced from country rocks immediately underlying the Platreef at several of these localities, the compositions of ore sulfides are next compared to those of country rocks at a more regional scale. This comparison can be made in order to determine whether magma transport during emplacement may have transported country rock sulfur from one region to another in a consistent fashion. The variations in isotopic composition can be compared to the inferred southward magma transport direction (Kinnaird et al., 2005).

Regional sedimentary country rocks exhibit a wide range of $\Delta^{33}S$ and $\delta^{34}S$ values (Fig. 2). The country-rock data can be grouped into three distinct categories: (1) a group with ^{34}S-depleted ($-35‰ \le \delta^{34}S \le -25‰$), mass dependently fractionated ($-0.20‰ \le \Delta^{33}S \le 0.25‰$) sulfur isotope compositions from southernmost Timeball Hill shales and siltstones; (2) a group with ^{34}S-enriched ($15‰ \le \delta^{34}S \le 42‰$), mass dependently fractionated ($-0.10‰ \le \Delta^{33}S \le 0.20‰$) sulfur isotope compositions from centrally located upper Duitschland carbonates; and (3) a group with moderately ^{34}S enriched, mass-independent sulfur isotope compositions from more northerly lower Duitschland shales and Malmani dolomites. A final northernmost country-rock type (basement granites) has not been measured for its multiple sulfur isotope compositions. Here we make the assumption (as described above) that the original $\delta^{34}S$ and $\Delta^{33}S$ values from these rocks are uniform and near zero.

Metamorphic rocks from the direct footwall to the Platreef and xenoliths within it show a narrower range in $\delta^{34}S$ values (–21 to 29‰) but more extended variability in $\Delta^{33}S$ values than the regional sedimentary country rocks (Fig. 2). These differences in composition are likely a reflection of original sedimentary heterogeneity. In general, the sulfur isotope compositions of the metamorphosed footwall rocks and xenoliths are consistent with the three groups identified above. Importantly, footwall and xenolith sulfur isotope compositions can be broadly predicted on the basis of their inferred protoliths. For example, the footwall contains calc-silicate and dolomite marbles that clearly originated either as Malmani dolomites (e.g., samples with high $\delta^{33}S$ values in Sandsloot cores) or siliceous carbonates from the upper Duitschland Formation (e.g., samples with high $\delta^{34}S$ and low $\Delta^{33}S$ values

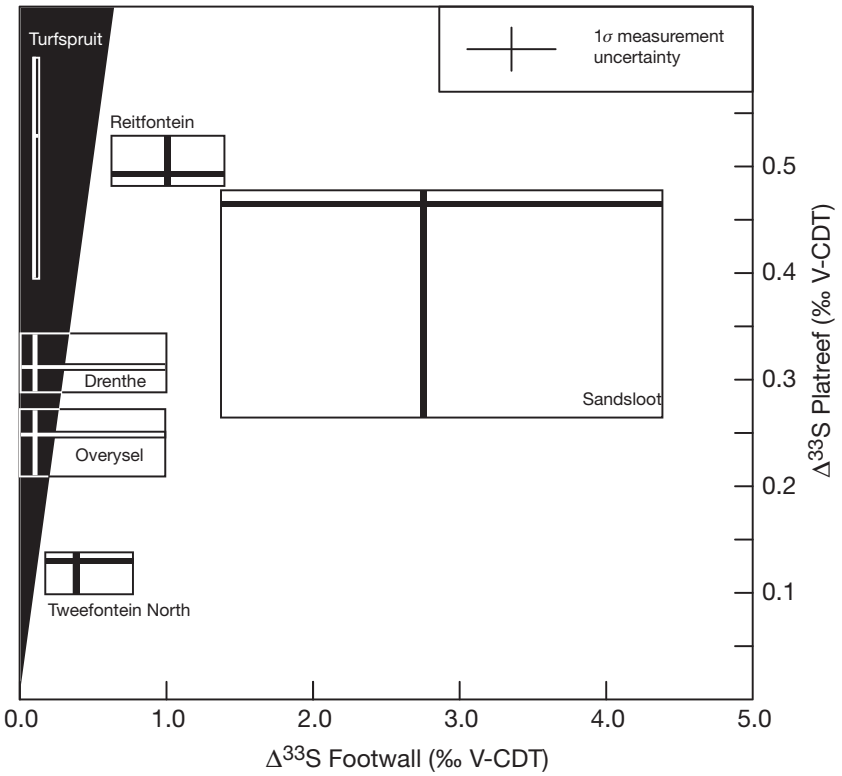

FIG. 3. Comparison of $\Delta^{33}S$ values of the Platreef and its direct footwall on different farms. Ranges represent 10th to 90th percentile of each grouping and intersect at the mode, reflecting the ore-footwall relationship characteristic of a given farm. Footwall $\Delta^{33}S$ values for Overysel and Drenthe are an estimated range from expected primary mantle values (~0‰; Farquhar et al, 2002) to average sedimentary sulfide for Archean (1‰; Johnston, 2011), allowing for the granitic footwall to range from an I- to an S-type granite. Platreef values intersect at the average value of unmineralized igneous rocks (Penniston-Dorland et al., 2008). Footwall $\Delta^{33}S$ values for Rietfontein are taken from the range of values measured in the equivalent country-rock protolith (lower Duitschland shales; Guo et al., 2009). Black filled triangle represents region where local contact enrichment of Platreef $\Delta^{33}S$ values is impossible.

in Turfspruit cores). Similarly, footwall and xenolith hornfels can be divided into those with protoliths from the lower Duitschland shales (e.g., samples with nonzero $\Delta^{33}S$ values in Tweefontein North cores), and those with affinities for the Timeball Hill shales (e.g., samples with negative $\delta^{34}S$ and low $\Delta^{33}S$ values in both Tweefontein North and Turfspruit cores). Original sedimentary sulfur isotope signatures have clearly been preserved through the contact metamorphic process, which suggests that a $\Delta^{33}S$-$\delta^{34}S$ plot may identify the ultimate sources of crustal sulfur in Platreef sulfides.

In strong contrast to the broad coverage exhibited by metamorphosed footwall rocks and xenoliths, Platreef ore sulfides occupy only the upper right quadrant on a $\Delta^{33}S$ versus $\delta^{34}S$ plot (Figs. 2, 4). Ore sulfides across the full reach of the Platreef have positive $\delta^{34}S$ and $\Delta^{33}S$ values, regardless of the underlying footwall rocks. These well-defined compositions were not simply inherited from the Platreef parental silicate melt, which was characterized by $\Delta^{33}S$ = 0.11 to 0.21‰ and $\delta^{34}S$ = 1.3 to 3.2‰ (Penniston-Dorland et al., 2008). Sulfur in the Platreef mineralizing system appears to reflect a common mixture. One end member was sulfur that has apparently equilibrated with the Platreef parental silicate melt. The other end members originated from restricted sedimentary horizons, most likely upper Duitschland carbonates and lower Duitschland shales (Figs. 2, 4). A contribution from the Malmani Dolomite cannot be ruled out isotopically, but the greater sulfide contents of the Duitschland Formation (Martini, 1979; Guo et al., 2009) suggest that it is a more likely source.

The abundant xenoliths in the Platreef could have acted as vehicles for spreading sulfur throughout the Platreef. However, these come mainly from the local footwall (Sharman-Harris et al., 2005) and generally preserve a sulfur isotope signature of their origin (Fig. 2). Xenolith-sourced sulfur is also not a likely explanation for the observations made here.

As the Platreef magma interacted with the local footwall, the isotopic signatures in the footwall rocks could have been transported "downstream." However, there does not appear to be a consistent advective offset toward the south between the isotopic composition of footwall rocks and Platreef sulfides (i.e., the inferred downstream direction during emplacement; Kinnaird et al., 2005). For example, sulfides from the most northerly localities (e.g., farms Drenthe and Overysel) preserve some of the largest $\delta^{34}S$ values (Table 1), suggesting greater contributions from some of the most southerly footwall rocks (i.e., upper Duitschland carbonates, Figs. 2, 4).

Coupled $\Delta^{33}S$-$\delta^{34}S$ constraints on preemplacement sulfur processing

Platreef ore sulfides do not appear to record the local sulfur isotope composition of the country rock, nor do they have

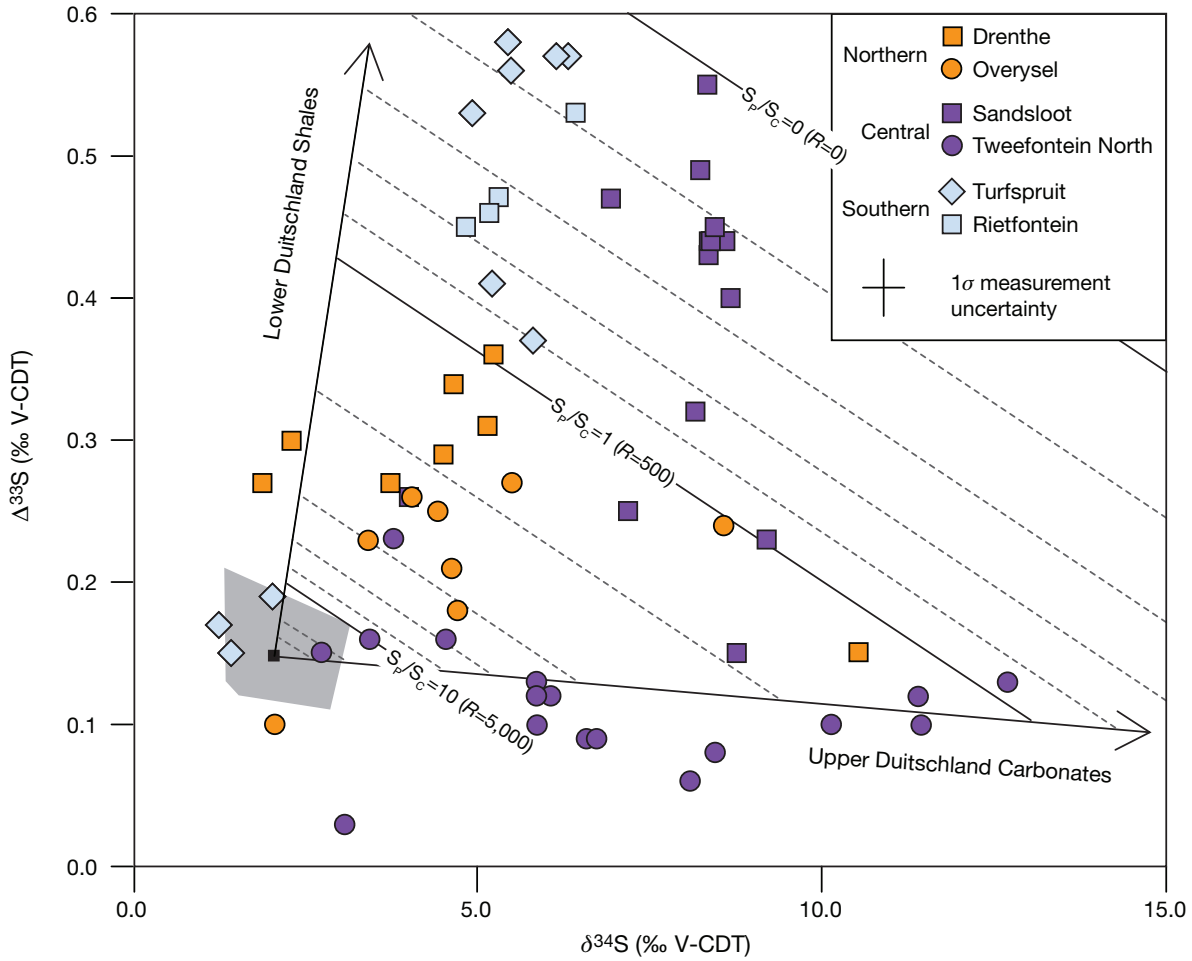

FIG. 4. Three-component mixing model for multiple sulfur isotope data from Platreef ore sulfides. Vectors point toward average multiple sulfur isotope compositions of lower Duitschland shales ($\Delta^{33}S$ = 0.706‰; $\delta^{34}S$ = 3.94‰) and upper Duitschland carbonates ($\Delta^{33}S$ = 0.055‰; $\delta^{34}S$ = 24.09‰). Gray field outlines region of $\Delta^{33}S$ and $\delta^{34}S$ values of unmineralized Platreef and Main zone igneous rocks (Penniston-Dorland et al., 2008). Diagonal lines are contours corresponding to different values of the sulfur mass fraction, S_P/S_C. The equivalent values of conventional *R* factors were calculated with equation 4 in the main text, and are shown here in parentheses.

any consistent offset of country-rock sulfur isotope compositions expected from magma transport in a single direction. The local addition of sulfur apparently made a minor contribution to the sulfur budget of the Platreef ore-forming system, despite evidence for assimilation of contact melts and isotopic redistribution through hydrothermal circulation (Holwell et al., 2007; Penniston-Dorland et al., 2008). With significant sulfur processing during and after emplacement ruled out, we suggest the Platreef magma was exposed to crustal material prior to its final emplacement.

Preemplacement crustal assimilation is also suggested by oxygen isotope measurements that indicate a greater amount of crustal oxygen in the Platreef than in the other rock types of the Bushveld (Harris and Chaumba, 2001). Detailed in situ $\delta^{34}S$ data also support sulfide saturation occurring prior to Platreef emplacement as well, suggesting incorporation of sulfur-rich crustal rocks (Holwell et al., 2007). Preemplacement crustal contamination of the Platreef magma has been identified in Re and Os data (Reisberg et al., 2011), with carbonaceous shales highlighted as a likely contaminant. Comparison of Platreef whole-rock CaO and FeO contents to PGE tenors and S/Se ratios suggests two phases of contamination of the Platreef magma, one prior to emplacement and one postemplacement (Ihlenfeld and Keays, 2011). When these numerous lines of evidence are taken together, a preemplacement influence on Platreef $\Delta^{33}S$ and $\delta^{34}S$ values is well supported.

Two lithologic units appear to control the $\Delta^{33}S$ and $\delta^{34}S$ values of the Platreef—upper Duitschland carbonates and lower Duitschland shales (Fig. 2). Their sulfur isotope compositions are well characterized (Guo et al., 2009), as is the sulfur isotope composition of the presumed Platreef parental melt (Penniston-Dorland et al., 2008). Here we adapt generalized mass balance expressions (Lesher and Burnham, 2001) to investigate how these potential end members set the final sulfur isotope distribution of the Platreef sulfides. Because the calculations are made for a closed system, they reflect the integrated history of interaction between the Platreef parental melt, contaminant-sourced sulfur, and the immiscible sulfide melt that formed the Platreef ore.

We use the following expressions to calculate the sulfur isotope consequences of closed-system interaction in the Platreef mineralizing system:

$$\Delta^{33}S_{PR} = \frac{\Delta^{33}S_C + \Delta^{33}S_P \times S_P/S_C}{1 + S_P/S_C} \quad (1)$$

and

$$\delta^{34}S_{PR} = \frac{\delta^{34}S_C + \delta^{34}S_P \times S_P/S_C}{1 + S_P/S_C}, \quad (2)$$

where the subscript "PR" refers to the immiscible sulfide melt that is now represented by the Platreef sulfides, the subscript "P" refers to the parental Platreef melt, the subscript "C" refers to contaminant added to the parental melt prior to contamination, and S_P/S_C is the mass ratio of sulfur from the parental melt relative to that from the contaminant (cf. R^* of Ripley and Li, 2003). In the case of a parental silicate melt and a coexisting contaminant sulfide melt, it is related to the conventional R factor (mass ratio of silicate melt to sulfide melt) by

$$S_P/S_C = R \times \frac{C_P^S}{C_C^S}, \quad (3)$$

where C_P^S is the concentration of sulfur in the parental silicate melt and C_C^S is the concentration of sulfur in the coexisting sulfide melt (Lesher and Burnham, 2001). We assume that mass-dependent sulfur isotope fractionation was negligible during preemplacement interaction (Ripley and Li, 2003). Although we recognize that sedimentary $\Delta^{33}S$ and $\delta^{34}S$ values are intrinsically variable (Guo et al., 2009), we use average sulfur isotope compositions from lower Duitschland shales ($\Delta^{33}S$ = 0.706‰; $\delta^{34}S$ = 3.94‰) and upper Duitschland carbonates ($\Delta^{33}S$ = 0.055‰; $\delta^{34}S$ = 24.09‰) in order to make our calculations. We represent the sulfur isotope composition of the Platreef parental melt as the average $\Delta^{33}S$ (0.15‰) and $\delta^{34}S$ (2.0‰) values of barren igneous rocks in the northern limb (Penniston-Dorland et al., 2008).

Our calculations show that Platreef ore sulfides reflect a broad range of S_P/S_C values, covering more than two orders of magnitude (Fig. 4). Although the absolute magnitudes of the S_P/S_C values depend on the specified isotopic compositions of the end members, their relative range is robust to these choices. There does not appear to be a relationship between the extent of contamination, as monitored by S_P/S_C values, and the proportion of contaminant from the lower Duitschland shales or the upper Duitschland carbonates (Fig. 4). Most of the Platreef sulfides preserve $\Delta^{33}S$ and $\delta^{34}S$ values that require contributions from both potential contaminants. The exception is the sulfide suite from Tweefontein North in the central sector. The Malmani Dolomite floors the central sector of the Platreef (Kinnaird et al., 2005), yet the Tweefontein North sulfides are dominated by sulfur contributions from rocks much higher in the footwall stratigraphy (upper Duitschland carbonates; Fig. 4). In addition, although there is clear evidence for a single contaminant at Tweefontein North, the degree of contamination is still extremely variable. Heterogeneous expression appears to be the rule for sulfur contamination within the Platreef.

This heterogeneity is shared by metal tenors measured from the Platreef (Kinnaird et al., 2005; Ihlenfeld and Keays, 2011). Variability in Cu contents and Pd contents in the Platreef produces silicate-sulfide melt mass ratios (R factors) that span two orders of magnitude (figs. 6, 8, Ihlenfeld and Keays, 2011). Because material exchange between coexisting silicate and sulfide melts can be recorded by sulfur isotopes (Ripley and Li, 2003), variable R factors could be a common explanation for the wide range of tenors and sulfur contamination in the Platreef. Our calculated S_P/S_C values are linearly related to R factors (equation 3), and can be interpreted as such under the assumption of isotopic equilibration between the final sulfide and silicate melts in the Platreef. If the average Platreef silicate magma had a sulfur concentration of ≈800 ppm by mass (Cawthorn, 2005) and the sulfur concentration in the sulfide melt was 38 wt % (Lesher and Burnham, 2001), then the following relationship between conventional R factors and values would hold:

$$R \approx 500 \times S_P/S_C. \quad (4)$$

The majority of the Platreef $\Delta^{33}S$ and $\delta^{34}S$ measurements would imply R factors from 0 to ≈5,000, with nearly 50% falling below R = 500 (S_P/S_C = 1, Fig. 4). This range barely overlaps with the range of R factors estimated from Cu and Pd, which fall mostly between 10^3 to 10^5 with a shallow tail down to ≈100 (Ihlenfeld and Keays, 2011).

Our calculations do not take into account the hydrothermal transfer of mass-independent wall-rock sulfur into the Platreef after emplacement. Such a process would lead to the contact enhancement of $\Delta^{33}S$ values in the Platreef ore sulfides, which, in turn, should result in artificially low R factor estimates. Hydrothermal sulfur transfer was apparently not an influential process across the whole of the Platreef as there is no correlation between Platreef $\Delta^{33}S$ values and those of their associated footwall (Fig. 3). Enhancement of Platreef $\Delta^{33}S$ values has been proposed within 5 m of the Platreef contact at Sandsloot and Tweefontein North (Penniston-Dorland et al., 2008). However, the R factors for both localities do not differ from the full range calculated here for the Platreef (Fig. 4), reaffirming that the effects of hydrothermal transfer are extremely localized and cannot be the reason for the small R factors inferred here.

It is well known that PGE reefs in layered intrusions require large R factors (Kerr and Leitch, 2005) to produce the observed high concentrations of PGEs. The reef-type deposits in the main Bushveld (Campbell et al., 1983; Naldrett et al., 2009) and those in the northern limb (Ihlenfeld and Keays, 2011) are not exceptions to this rule. The presence of sulfur isotope anomalies in the Platreef suggests R factors were orders of magnitude lower than was previously calculated based on metal contents. This mismatch highlights the fundamental issue identified in this study: how can contaminant sulfur multiple isotope signatures be preserved in the face of the very high R factors demanded by the metal tenors of the Platreef? At R factors of 10^4, even extremely sulfur poor silicate magmas will dilute the $\Delta^{33}S$ values in a coexisting sulfide melt to less than 20% of their original values (Fiorentini et al., 2012). Negligible traces of the original $\Delta^{33}S$ value of the contaminant will survive at R factors of 10^5 (Fiorentini et al., 2012). In the next section we discuss some possible solutions to this puzzle.

Reconciling signatures of Platreef mineralization

We offer a pair of possibilities for reconciling the discrepancy identified above. The first possibility takes the point of view that metals and the $\Delta^{33}S_P$ and $\delta^{34}S_P$ values were carried by a parental silicate melt (undersaturated with respect to sulfide). Prior to emplacement in the Platreef, this parental silicate melt could have assimilated sulfur from the Duitschland Formation. If sulfur solubility in the silicate melt were exceeded, an immiscible sulfide melt would segregate after assimilation. Alternatively, an initial sulfide melt ("xenomelt," Lesher and Burnham, 2001) could have derived from partial melting of sulfide-rich horizons in the Duitschland Formation prior to mixing with the parental silicate melt. Whether an immiscible sulfide melt exsolved from the silicate melt or was extracted from wall rocks, it would have carried an isotopic signature of the contaminating sulfur. As the silicate melt interacted with the immiscible sulfides, metals would be partitioned into the sulfide melt (Campbell and Naldrett, 1979). Concurrent sulfur isotope exchange would draw the crustal $\Delta^{33}S$ and $\delta^{34}S$ values of the contaminant sulfide toward those of the parental silicate melt (Ripley and Li, 2003; Fiorentini et al., 2012). Because of the relatively low sulfur concentration of silicate melts, this process would lead to a conventional *R* factor interpretation of the S_P/S_C values calculated here. An abnormally Ni, Cu, and PGE rich parental silicate melt would be needed to equalize the isotope- and metal-based *R* factors calculated for the Platreef. Recent geochemical modeling of the Merensky Reef has relied on such a melt (Naldrett et al., 2009), which may have escaped from the main Bushveld Basin through the northern limb (Naldrett et al., 2011).

A second possibility considers that metals and the $\Delta^{33}S_P$ and $\delta^{34}S_P$ values were hosted by a preexisting parental sulfide melt entrained in a silicate melt partner. Under this interpretation, the silicate melt would have been sulfur saturated prior to interaction with the Duitschland Formation and prior to emplacement in the Platreef. In addition, the coexisting sulfide melt would have carried elevated Ni, Cu, and PGE abundances due to an earlier stage of interaction with a silicate melt. Although such a saturated system would not have driven sulfur assimilation, sulfide xenomelts could have resulted from partial melting of sulfide-rich wall rocks from the Duitschland Formation. The $\Delta^{33}S$ and $\delta^{34}S$ systematics of Platreef sulfides in Figure 4 suggest that such xenomelts would have been variably mixed with the parental sulfide melt prior to emplacement of the Platreef. From this perspective, the S_P/S_C values calculated here are mass ratios of sulfur from each component, since both sulfide melts would have the same approximate sulfur concentration. As the S_P/S_C values approach zero, the sulfur isotope signature of the parental sulfide melt would be overwhelmed by the crustal isotope anomalies within the xenomelt. Because the sulfide xenomelt would not be as metal rich as the parental sulfide, any elevated Ni, Cu, and PGE abundances carried by the parental sulfide would be diminished proportionally. Lithologic, geochemical, and stratigraphic similarities have long led to the suggestion that the Platreef sulfide ore is the northern limb analogue to the Merensky Reef ore horizon (see discussion in Kinnaird et al., 2005). Recent proposals suggest that they formed from the same PGE-rich silicate melt (Naldrett et al., 2011). A common origin for the parental Platreef sulfide melt and the immiscible sulfide melt now represented by the Merensky Reef is apparently not an unreasonable possibility.

There is some isotopic support for both possibilities discussed above. Outside of mineralized zones, the $\Delta^{33}S$ and $\delta^{34}S$ values of the Platreef are remarkably homogeneous at $\Delta^{33}S = 0.15 \pm 0.04$ ‰ (1σ) and $\delta^{34}S = 2.0 \pm 0.8$ ‰ (1σ) (Penniston-Dorland et al., 2008). These compositions overlap closely with $\Delta^{33}S$ and $\delta^{34}S$ values from Merensky Reef ore and associated silicate rocks (Penniston-Dorland et al., 2012). One argument in favor of the second possibility is that it seems to require fewer processes. In particular, it calls for a single Ni, Cu, and PGE enrichment event for both the Merensky Reef and Platreef, neatly explaining their similarly high maximum metal tenors despite their different environments of formation. A parental sulfide melt to the Platreef would carry a record of the high *R* factors seen in the Merensky Reef (Campbell et al., 1983; Naldrett et al., 2009), providing a viable mechanism for the maximum *R* factors observed in the Platreef (Ihlenfeld and Keays, 2011). The present variability in Platreef *R* factors might be a simple artifact of heterogeneous mixing of the parental sulfide melt with a xenomelt derived from the Duitschland Formation. The Platreef $\Delta^{33}S$ and $\delta^{34}S$ values suggest that the mass ratio of parental sulfide to xenomelt sulfide ranged from <0.1 to >10 (Fig. 4). The accompanying dilution of the metal-rich parental sulfide could cause the observed two orders of magnitude variation in metal-based Platreef *R* factors (Ihlenfeld and Keays, 2011). Sulfide mixing could also give rise to the observed inverse correlation of metal-based *R* factors in the Platreef with other potential indicators of sedimentary contamination (e.g., S-Se ratios; Ihlenfeld and Keays, 2011). A prediction of the mixing model is that a similar inverse correlation should exist between PGE abundances (as proxies for *R* factor) and the magnitude of $\Delta^{33}S$ and $\delta^{34}S$ values in Platreef ore sulfide. Identification of such a local correlation would require a coupled study of metal tenors and sulfur isotopes on the same samples. Whereas the above argument is based on parsimony, extremely PGE rich magmatic sulfide inclusions have recently been found in Platreef chromite grains (Holwell et al., 2011), pointing to a physical record of a metal-rich preemplacement parental sulfide melt.

Locus and mechanism of preemplacement sulfur assimilation

Whether or not the parental Platreef silicate melt was sulfur saturated prior to emplacement, our sulfur isotope measurements can speak to the locus and mechanism of preemplacement crustal assimilation. The Platreef intruded into sedimentary rocks of the upper Transvaal Supergroup as several pulses of magma rather than one individual event (Kinnaird, 2005). Sulfur contamination prior to emplacement originated from the Duitschland Formation, which occupies only a narrow window of the upper Transvaal Supergroup stratigraphy. Before emplacement, each pulse of Platreef magmas must have resided in spatially restricted staging chambers bounded by rocks of the Duitschland Formation. These characteristics are consistent with the "pudding basin model" of the Bushveld Complex, where the northern limb

represents an intermittent escape route for overpressured Bushveld magmas between two nested basins of similar size (Naldrett et al., 2008). If the contact point between the two basins were in the Duitschland Formation, then floor and roof rocks of the right affinity would have constantly surrounded the ponded magma. The length of time the magma spent behind this "Duitschland dam" would presumably control the extent of sulfur extraction from the surrounding host rocks. Sporadic development of magmatic overpressures would lead to variability in residence times, naturally giving rise to heterogeneous contamination of the Platreef magma by crustal sulfur. Crustal sulfur assimilation is often thought to initiate the ore-forming process by producing an immiscible sulfide melt that can collect base metals and PGEs. In the Platreef, however, crustal sulfur assimilation apparently diluted a preexisting PGE-rich sulfide melt instead.

Acknowledgments

We would like to thank Louis Schurmann and David Broughton of Ivanhoe Nickel and Platinum Ltd.; Gernot Wober and Hunter Dickinson/Anooraq Resources; and Gordon Chunnett and AngloPlatinum for providing access to samples and data for this study. ERS was supported by a Society of Economic Geologists Graduate Student Fellowship, a GEOTOP bourses d'études des cycles supérieurs, and an NSERC Discovery Grant to BAW. Research costs were covered by an NSERC Discovery Grant to BAW. Initial funding for this project was provided to JAK by the South African Technology and Human Resources for Industry Programme and to SP-D, MB, and BAW by U.S. Geological Survey Mineral Resources External Research Program (MRERP) Grant 05HQGR0158. Access to the University of Maryland Stable Isotope Laboratory was provided by kind permission of James Farquhar, director. We thank Marco Fiorentini for his constructive review and associate editor Steve Barnes for his lucid and generous guidance as we explored the implications of our measurements for PGE mineralization processes in the Platreef.

REFERENCES

Armitage, P.E.B., McDonald, I., Edwards, S.J., and Manby, G.M., 2002, Platinum-group element mineralization in the Platreef and calc-silicate footwall at Sandsloot, Potgietersrus district, South Africa: Transactions of the Institute of Mining and Metallurgy, v. 111, p. B36–B45.

Barton, Jr., J.M., Cawthorn, R.G., and White, J., 1986, The role of contamination in the evolution of the Platreef of the Bushveld Complex: Economic Geology, v. 81, p. 1096–1104.

Bekker, A., Holland, H.D., Wang, P.L., Rumble, D., Stein, H.J., Hannah, J.L., Coetzee, L.L., and Beukes, N.J., 2004, Dating the rise of atmospheric oxygen: Nature, v. 427, p. 117–120.

Bekker, A., Barley, M.E., Fiorentini, M.L., Rouxel, O.J., Rumble, D., and Beresford, S.W., 2009, Atmospheric sulfur in Archaean komatiite-hosted nickel deposits: Science, v. 326, p. 1086–1089.

Buchanan, D.L., and Rouse, J.E., 1984, Role of contamination in the precipitation of sulfides in the Platreef of the Bushveld Complex, *in* Buchanan, D.L., and Jones, M.J., eds., Sulfide deposits in mafic and ultramafic rocks: London, Institute of Mining and Metallurgy, p. 141–146.

Buchanan, D.L., Nolan, J., Suddaby, P., Rouse, J.E., Viljoen, M.J., and Davenport, J.W.J., 1981, The genesis of sulfide mineralization in a portion of the Potgietersrus limb of the Bushveld Complex: Economic Geology, v. 76, p. 568–579.

Campbell, I.H., and Naldrett, A.J., 1979, The influence of silicate:sulfide ratios on the geochemistry of magmatic sulfides: Economic Geology, v. 74, p. 1503–1506.

Campbell, I.H., Naldrett, A.J., and Barnes, S.J., 1983, A model for the origin of the platinum-rich sulfide horizons in the Bushveld and Stillwater Complexes: Journal of Petrology, v. 24, p. 133–160.

Canfield, D.E., Raiswell, R., Westrich, J.T., Reaves, C.M., and Berner, R.A., 1986, The use of chromium reduction in the analysis of reduced inorganic sulfur in sediments and shales: Chemical Geology, v. 54, p. 149–55.

Cartigny, P., Farquhar, J., Thomassot, E., Harris, J.W., Wing, B., Masterson, A., McKeegan, K., and Stachel, T., 2009, A mantle origin for Paleoarchean peridotitic diamonds from the Panda kimberlite, Slave craton: Evidence from ^{13}C-, ^{15}N- and $^{33,34}S$-stable isotope systematics: Lithos, v. 112S, p. 852–864.

——2005, Contrasting sulphide contents of the Bushveld and Sudbury Igneous Complexes: Mineralium Deposita, v. 40, p. 1–12.

Coetzee, L.L., 2001, Genetic stratigraphy of the Paleoproterozoic Pretoria Group in the western Transvaal: Unpublished M.Sc. Thesis, Johannesburg, South Africa, Rand Afrikaans University, 212 p.

Danielache, S.O., Eskebjerg, C., Johnson, M.S., Ueno, Y., and Yoshida, N., 2008, High-precision spectroscopy of ^{32}S, ^{33}S, and ^{34}S sulfur dioxide: Ultraviolet absorption cross sections and isotope effects: Journal of Geophysical Research, v. 113, D17314, 14 p.

Ding, X., Ripley, E.M., Shirey, S.B., and Li, C., 2011, Os, Nd, O and S isotope constraints on country rock contamination in the conduit related Eagle Cu-Ni-(PGE) deposit, Midcontinent rift system, upper Michigan: Geochimica et Cosmochimica Acta, in press.

Eriksson, P.G., Altermann, W., Catuneanu, O., van der Merwe, R., and Bumby, A.J., 2001, Major influences on the evolution of the 2.67 – 2.1 Ga Transvaal Basin, Kaapvaal craton: Sedimentary Geology, v. 141–142, p. 205–231.

Farquhar, J., and Wing, B.A., 2003, Multiple sulphur isotopes and the evolution of the atmosphere: Earth and Planetary Science Letters, v. 213, p. 1–13.

Farquhar, J., Savarino, J., Airieau, S., and Thiemens, M.H., 2001, Observation of wavelength-sensitive mass-independent sulfur isotope effects during SO_2 photolysis: Implications for the early atmosphere: Journal of Geophysical Research, v. 106, p. 32,829–32,839.

Farquhar, J., Wing, B., McKeegan, K., Harris, J., Cartigny, P., and Thiemens, M., 2002, Mass-independent sulfur of inclusions in diamond and sulfur recycling on early earth: Science, v. 298, p. 2369–2372.

Fiorentini, M.L., Bekker, A., Rouxel, O., Wing, B.A., Maier, W., and Rumble, D., 2012, Multiple sulfur and iron isotope composition of magmatic Ni-Cu-(PGE) sulfide mineralization from eastern Botswana: Economic Geology, v. 107, p. 105–116

Fleet, M.E., Crocket, J.H., Liu, M., and Stone, W.E., 1999, Laboratory partitioning of platinum-group elements (PGE) and gold with application to magmatic sulfide-PGE deposits: Lithos, v. 47, p. 127–142.

Guo, Q., Strauss, H., Kaufman, A.J., Schroeder, S., Gutzmer, J., Wing, B., Baker, M.A., Bekker, A., Jin, Q., Kim, S., and Farquhar, J., 2009, Reconstructing Earth's surface oxidation across the Archean-Proterozoic transition: Geology, v. 37, p. 399–402.

Harris, C., and Chaumba, J.B., 2001, Crustal contamination and fluid-rock interaction during the formation of the Platreef, northern limb of the Bushveld Complex, South Africa: Journal of Petrology, v. 42, p. 1321–1347.

Holwell, D.A., and McDonald, I., 2006, Petrology, geochemistry and the mechanisms determining the distribution of platinum group element and base metal sulfide mineralization in the Platreef at Overysel, northern Bushveld Complex, South Africa: Mineralium Deposita, v. 41, p. 575–598.

Holwell, D.A., Boyce, A.J., and McDonald, I., 2007, Sulfur isotope variations within the Platreef Ni-Cu-PGE deposit: Genetic implications for the origin of sulfide mineralization: Economic Geology, v. 102, p. 1091–1110.

Holwell, D.A., McDonald, I., and Butler, I.B., 2011, Precious metal enrichment in the Platreef, Bushveld Complex, South Africa: Evidence from homogenized magmatic sulfide inclusions: Contributions to Mineralogy and Petrology, v. 161, p. 1011–1026.

Hu, G., Rumble, D., and Wang, P., 2003, An ultraviolet laser microprobe for the in situ analysis of multisulfur isotopes and its use in measuring Archean sulfur isotope mass-independent anomalies: Geochimica et Cosmochimica Acta, v. 67, p. 3101–3117.

Hulbert, L.J., 1983, A petrographical investigation of the Rustenburg Layered Suite and associated mineralization south of Potgietersrus: Unpublished D.Sc. dissertation, Pretoria, South Africa, University of Pretoria, 511 p.

Hutchinson, D., and Kinnaird, J.A., 2005, Complex multi-stage genesis for the Ni-Cu-PGE mineralization in the southern region of the Platreef,

Bushveld Complex, South Africa: Transactions of the Institute of Mining and Metallurgy, v. 114, p. B208–B224.
Hutchinson, D., and McDonald, I., 2008, Laser ablation ICP-MS study of platinum-group elements in sulphides from the Platreef at Turfspruit, northern limb of the Bushveld Complex, South Africa: Mineralium Deposita, v. 43, p. 695–711.
Ihlenfeld, C., and Keays, R.R., 2011, Crustal contamination and PGE mineralization in the Platreef, Bushveld Complex, South Africa: Evidence for multiple contamination events and transport of magmatic sulfides: Mineralium Deposita, v. 46, p. 813–832.
Jamieson, J.W., Wing, B.A., Hannington, M.D., and Farquhar, J., 2006, Evaluating isotopic equilibrium among sulfide mineral pairs in Archean ore deposits: Case study from the Kidd Creek VMS deposit, Ontario, Canada: Economic Geology, v. 101, p. 1055–1061.
Johnston, D.T., 2011, Multiple sulfur isotopes and the evolution of Earth's surface sulfur cycle: Earth-Science Reviews, v. 106, p. 161–183.
Johnson, T.E., Brown, M., and White, R.W., 2010, Partial melting of metapelitic xenoliths within the southern Platreef, Bushveld Complex, South Africa: Journal of Metamorphic Geology, v. 28, p. 269–291.
Kerr, A., and Leitch, A.M., 2005, Self-destructive segregation systems and the formation of high-grade magmatic ore deposits: Economic Geology, v. 100, p. 311–332.
Kinnaird, J.A., 2005, Geochemical evidence of multiphase emplacement in the southern Platreef: Transactions of the Institute of Mining and Metallurgy, v. 114, p. B225–B242.
Kinnaird, J.A., Hutchinson, D., Schurmann, L., Nex, P.A.M., and de Lange, R., 2005, Petrology and mineralization of the southern Platreef: Northern limb of the Bushveld Complex, South Africa: Mineralium Deposita, v. 40, p. 476–597.
Lesher, C.M., and Burnham, O.M., 2001, Multicomponent elemental and isotopic mixing in Ni-Cu-(PGE) ores at Kambaldo, Western Australia: Canadian Mineralogist, v. 39, p. 421–446.
Liebenberg, L., 1968, The sulphides in the layered sequence of the Bushveld Igneous Complex: Unpublished D.Sc. Thesis, Pretoria, South Africa, University of Pretoria, 260 p.
Lyons, J.R., 2007, Mass-independent fractionation of sulfur isotopes by isotope-selective photodissociation of SO_2: Geophysical Research Letters, v. 34, L22811, 5 p.
Manyeruke, T.D., Maier, W.D., and Barnes, S-J., 2005, Major and trace element geochemistry of the Platreef on the farm Townlands, northern Bushveld Complex: South African Journal of Geology, v. 108, p. 381–396.
Martini, J.E.J., 1979, A copper-bearing bed in the Pretoria Group in the northeastern Transvaal, *in* Anderson, A.L., van Biljoen, W.J., eds., Some sedimentary basins and associated ore deposits of South Africa: Geological Society of South Africa Special Publication 6, p. 65–72.
Mungall, J.E., 2002, Kinetic controls on the partitioning of trace elements between silicate and sulfide liquids: Journal of Petrology, v. 43, p. 749–768.
Mungall, J.E., and Naldrett, A.J., 2008, Ore deposits of the platinum-group elements: Elements, v. 4, p. 253–258.
Naldrett, A.J., 2004, Magmatic sulfide deposits geology, geochemisty and exploration: Berlin, New York, Springer, 727 p.
——2010, Secular variation of magmatic sulfide deposits and their source magmas: Economic Geology, v. 105, p. 669–688.
Naldrett, A., Kinnaird, J., Wilson, A., and Chunnett, G., 2008, Concentration of PGE in Earth's crust with special reference to the Bushveld Complex: Earth Science Frontiers, v. 15, p. 264–297.
Naldrett, A.J., Wilson, A., Kinnaird, J., and Chunnett, G., 2009, PGE tenor and metal ratios within and below the Merensky Reef, Bushveld Complex: Implications for its genesis: Journal of Petrology, v. 50, p. 625–659.
Naldrett, A., Kinnaird, J., Wilson, A., Yudovskaya, M., and Chunnett, G., 2011, Genesis of the PGE-enriched Merensky Reef and chromitite seams of the Bushveld Complex: Reviews in Economic Geology, v. 17, p. 235–296.
Ono, S., Shanks, III, W.C., Rouxel, O.J., and Rumble, D., 2007, S-33 constraints on the seawater sulfate contribution in modern seafloor hydrothermal vent sulfides: Geochimica et Cosmochimica Acta, v. 71, p. 1170–1182.
Penniston-Dorland, S.C., Wing, B.A., Nex, P.A.M., Kinnaird, J.A., Farquhar, J., Brown, M., and Sharman, E.R., 2008, Multiple sulfur isotopes reveal a primary magmatic origin for the Platreef PGE deposit, Bushveld Complex, South Africa: Geology, v. 36, p. 979–982.
Penniston-Dorland, S.C., Mathez, E.A., Wing, B., Farquhar, J., and Kinnaird, J.A., 2012, Multiple sulfur isotope evidence for surface-derived sulfur in the Bushveld Complex: Earth and Planetary Science Letters, v. 337–338, p. 236–242.
Peters, M., Strauss, H., Farquhar, J., Ockert, C., Eickmann, B., and Jost, C.L., 2010, Sulfur cycling at the Mid-Atlantic Ridge: A multiple sulfur isotope approach: Chemical Geology, v. 269, p. 180–196.
Reisberg, L., Tredoux, M., Harris, C., Coftier, A., and Chaumba, J., 2011, Re and Os distribution and Os isotope composition of the Platreef at the Sandsloot-Mogolakwena Mine, Bushveld Complex, South Africa: Chemical Geology, v. 281, p. 352–363.
Ripley, E., and Li, C., 2003, Sulfur isotope exchange and metal enrichment in the formation of magmatic Cu-Ni-(PGE) deposits: Economic Geology, v. 98, p. 635–641.
Robinson, B.W., 1995, Sulphur isotope standards: International Atomic Energy Agency TECDOC 825, p. 39–45.
Rouxel, O., Ono, S., Alt, J., Rumble, D., and Ludden, J., 2008, Sulfur isotope evidence for microbial sulfate reduction in altered oceanic basalts at ODP Site 801: Earth and Planetary Science Letters, v. 268, p. 110–123.
Seal, R., 2006, Sulfur isotope geochemistry of sulfide minerals: Reviews in Mineralogy and Geochemistry, v. 61, p. 633–677.
Sharman-Harris, E., Kinnaird, J.A., Harris, C., and Horstmann, U.E., 2005, A new look at sulfide mineralization of the northern limb, Bushveld Complex: A stable isotope study: Transactions of the Institute of Mining and Metallurgy, v. 114, p. B252–B263.
Watanabe, Y., Farquhar, J., and Ohmoto, H., 2009, Anomalous fractionations of sulfur isotopes during thermochemical sulfate reduction: Science, v. 324, p. 370–373.